JOURNAL OF MATERIALS SCIENCE 32 (1997) 2753–2758

# Crack formation in mesophase pitch-based carbon fibres

## Part I *Some influential factors for crack formation*

SEONG-HO YOON, NOBUYUKI TAKANO*, YOZO KORAI, ISAO MOCHIDA
*Institute of Advanced Material Study, Department of Molecular Science and Technology and*
** Graduate School of Engineering Sciences, Kyushu University, Kasuga Fukuoka 816, Japan*

The crack observable in the transverse section of mesophase pitch-based graphitized fibres was studied to clarify its development on spinning, stabilization, carbonization and graphitization, and to find the factors influential on the development on spinning. The crack was already observed as an embryo in the as-spun fibre of radial texture, which increased the opening angle according to the extent of shrinkage due to carbonization and graphitization. The spinning temperature, length/diameter, diameter and wall material of the spinning nozzle and the kind of mesophase pitch were found influential in crack development, defining the transverse texture and the extent of longitudinal alignment along the fibre axis. Although the radial texture defined under an optical microscope tends to give a crack, not all of such textures carried the crack, suggesting the necessity of more detailed classification of the texture in terms of alignment, shape and size of domains observed under high resolution scanning electron microscopy (HR-SEM). The factors revealed as being influential on the textures appear to be related to the apparent viscosity, the perfectness of the radial orientation and die-swelling at the outlet of the nozzle to modify the texture defined through the nozzle. The interaction of the mesophase pitch with the nozzle wall and flow properties should be emphasized as factors controlling the texture on spinning.

## 1. Introduction

Mesophase pitch-based carbon fibres of high performance in their strengths and thermal conductivities have been recognized for some time as structural materials for the next century. The control of their micro- and macroscopic structures appears to be the most important key to obtaining high performances.

Crack formation has often been observed in the transverse sections of the fibres of radial texture along the fibre axis [1]. Since such a crack markedly reduces the strength, it is required to clarify the mechanism and influences of spinning conditions on crack formation. It has been reported that fibres spun through a large length/diameter ($L/D$) nozzle [2] over a particular range of temperatures [3] carried cracks. The present authors have reported that the viscosity controllable by blending is very influential on the transverse texture of the fibre [4]. Thus, several factors included in spinning appear to be influential on crack formation.

In the present study, the carbon fibres were produced from two kinds of mesophase pitches through SUS-304 and graphite spinning nozzles of various diameters at several temperatures to clarify the influences of spinning conditions in a broad sense on the development of the radial texture and crack in the transverse section of the mesophase pitch-based carbon fibre.

## 2. Experimental procedure

### 2.1. Materials

Some properties of the mesophase pitches used in this study are summarized in Table I. They were prepared from naphthalene (NP) and methyl naphthalene (mNP) with $HF/BF_3$ catalyst (Mitsubishi Gas Chemical Co.) [5, 6]. Mesophase pitch from C9 hydrocarbons, prepared by Mitsubishi Oil Co. [7], was also used for the control of transverse texture.

### 2.2. Spinning of the mesophase pitches

Spinning spinnerets with different sizes and materials which were used in this study are listed in Table II. Fig. 1 shows schematically the round, slit and Y-shaped spinning spinnerets. Mesophase pitch was extruded from the spinning spinneret under pressurized nitrogen, using a laboratory-scaled monofilament spinning apparatus [8], elongated by winding into pitch fibres of 10–15 μm in diameter. Detailed spinning conditions are summarized in Table III.

### 2.3. Stabilization and carbonization of the pitch fibres

Oxidative stabilization of the pitch fibres was carried out at 250 °C at a heating rate of 1.5 °C min$^{-1}$ for

0022–2461  

TABLE I Some analytical properties of mesophase pitches prepared from aromatic hydrocarbons

| Code | Raw material | SP[a] (°C) | AC[b] (vol %) | Solubilities (wt %) | | | $H/C$ | fa[c] | X-ray properties | |
|---|---|---|---|---|---|---|---|---|---|---|
| | | | | BS | BI-PS | PI(QI) | | | $d_{002}$ (nm) | $Lc_{(002)}$ (nm) |
| mNP | Methylnaphthalene | 205 | 100 | 52 | 19 | 33(29) | 0.69 | 0.81 | 0.3524 | 7.5 |
| NP | Naphthalene | 240 | 100 | 33 | 19 | 48(31) | 0.62 | 0.80 | 0.3574 | 3.2 |
| C9P | C9 hydrocarbons | 197 | 100 | 53 | 23 | 26 | 0.71 | 0.80 | 0.3512 | 4.2 |

[a] Softening point; [b] anisotropic contents; [c] carbon aromaticity.

TABLE II Spinning spinnerets used in this study

| Shape | Material | Aspects of the capillary | | Code |
|---|---|---|---|---|
| | | Length/Diameter ($L/D$) | Diameter (mm) | |
| Round | SUS-304 | 1 | 0.3 | SUS-R(1)-0.3 |
| | | 3 | 0.3 | SUS-R(3)-0.3 |
| | | | 0.5 | SUS-R(3)-0.5 |
| | Graphite[a] | 3 | 0.3 | Gra-R-0.3 |
| | | | 0.5 | Gra-R-0.5 |
| Slit | SUS-304 | $0.1 \times 0.7$ mm | | Slit |
| Y | SUS-304 | Length and width of a lobe, 0.3 and 0.2 mm, respectively | | Y |

[a] Density, 2.14 g cm$^{-3}$.

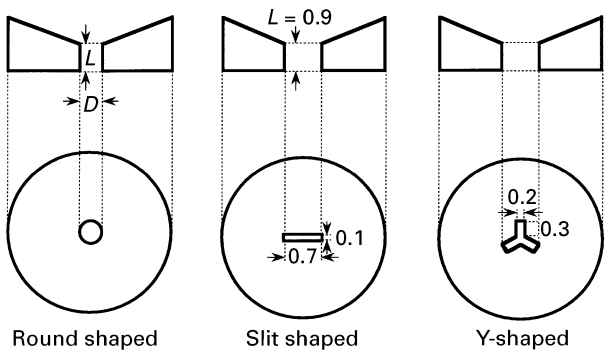


*Figure 1* Schematic pictures of spinning spinnerets used in this study.

20 min in air. The stabilized fibres were successively carbonized at 1300 °C at a heating rate of 10 °C min$^{-1}$ for 1 h in an Ar atmosphere. Graphitization was conducted at 2500 °C for 1 h at a heating rate of 100 °C min$^{-1}$ in an Ar atmosphere.

## 2.4. Characterization of the fibres

The transverse sections of the fibres were observed on a polarized microscope (Olympus BH2) and a scanning electron microscope (Jeol JSM-5400).

The degree of preferred orientation along the fibre axis of the fibres were measured and calculated from the half-width at half-maximum intensity (HWHM) of the (0 0 2) arc according to the method defined by Gakushin [9], using a wide-angled X-ray diffractometer (Rigaku Geigerflex; Cu$K_\alpha$, 0.15406 nm, 40 kV, 30 mA).

# 3. Results

## 3.1. Steps for crack formation and development

Fig. 2 shows the open crack development in the fibres from mNP spun through an SUS round-shaped nozzle of $L/D = 3$. The transverse texture of the pitch

TABLE III Spinning conditions

| Code | Mesophase pitch | Spinning temperature (°C) | Diameter of fibres (μm) |
|---|---|---|---|
| SUS-R(1)-0.3 | mNP | 265–290 | 9.0 ( ± 1.2) |
| SUS-R(3)-0.3 | mNP | 265–290 | 8.0 ( ± 0.8) |
| SUS-R(3)-0.5 | mNP | 270–290 | 8.5 ( ± 1.8) |
| Gra-R-0.3 | mNP | 270–290 | 8.5 ( ± 2.0) |
| Gra-R-0.5 | mNP | 270–290 | 8.5 ( ± 1.6) |
| Slit | mNP | 275 | – |
| Y | mNP | 275 | – |
| SUS-R(3)-0.3 | NP | 285 | 8.1 ( ± 0.8) |
| SUS-R(3)-0.3 | mNP/C9 | 285 | 9.2 ( ± 1.2) |

Spinning rate, 400 m min$^{-1}$; amount of extrudate, ca. 80 mg min$^{-1}$.

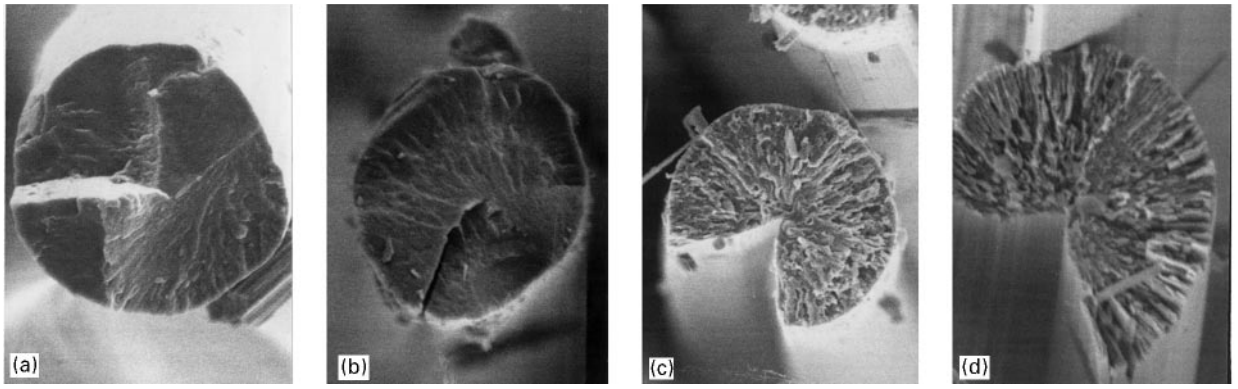


*Figure 2* Development of the open crack with increasing heat treatment temperature. Fibre: (a) spun; (b) stabilized; (c) carbonized; (d) graphitized.

fibre exhibited an embryo of the crack. The open angle of the crack increased with successive heat treatments, being ca. 10° after stabilization (Fig. 2a), 60° after carbonization (Fig. 2b) and 120° after graphitization (Fig. 2c). It is definite that carbonization and graphitization enlarge the opening angles of cracks.

## 3.2. Influences of spinning conditions on crack formation

### *3.2.1. L/D ratio of spinning nozzle and spinning temperature*

Fig. 3 shows the transverse textures of graphitized fibres from mNP spun through round-shaped SUS nozzles of $L/D = 1$ and 3, and $D = 0.3$ mm at 265–285 °C. Carbon fibres spun through the round-shaped nozzle of $L/D = 1$ showed radial skin-random core structures with no cracks in the transverse sections regardless of spinning temperature. Transverse textures of the carbon fibres spun with a nozzle of $L/D = 3$ provided a typical radial open crack by spinning at 275–285 °C. However, carbon fibres spun through the same nozzle $> 290$ °C showed no crack in the skin-onion textures. The nozzle of $L/D = 3$ but $D = 0.5$ mm provided a kind of radial texture, however, no crack was found, regardless of the spinning temperature, as shown in Fig. 4.

### *3.2.2. Wall materials and dimensions of the spinning nozzle*

Fig. 4 shows the transverse sections of carbon fibres from mNP spun through the round-shaped graphite nozzles of $L/D = 3$, and $D = 0.3$ and 0.5 mm. The transverse textures of the graphitized fibres spun through the graphite nozzles showed kinds of radial structures, nevertheless, no cracks were observed. Cracks appeared to be observed in the radial texture of particular types, which need more detailed definitions.

## 3.3. Shape of the fibre

Fig. 5 shows the transverse textures of the graphitized fibres from mNP spun through the round ($L/D = 3$,

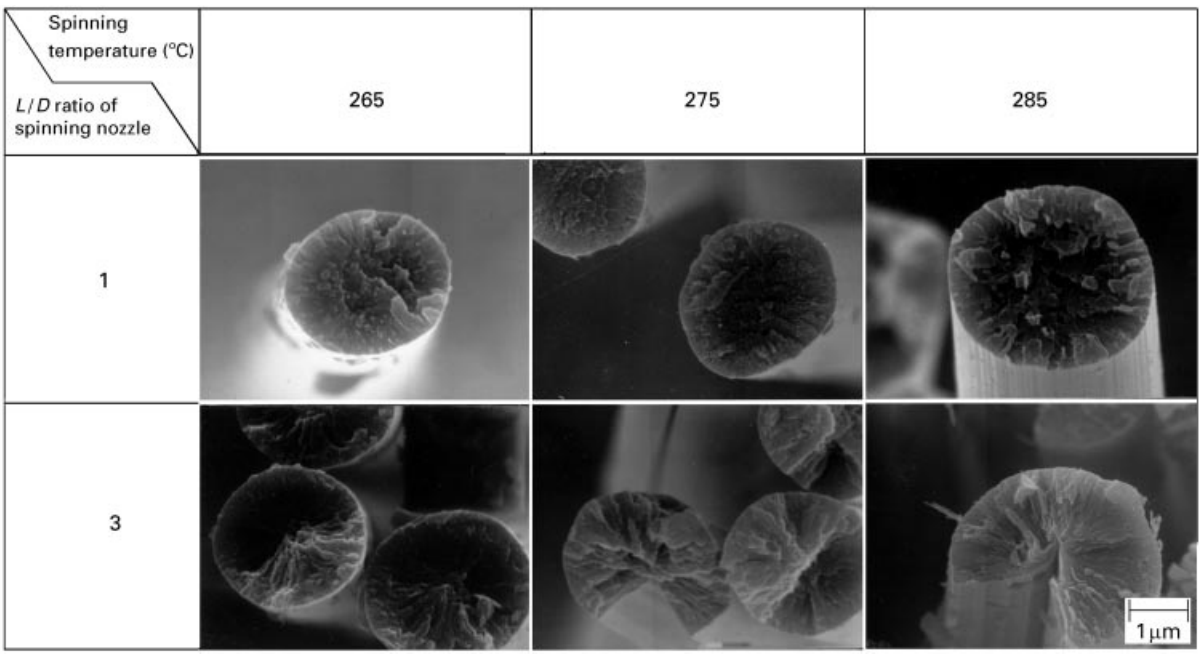


*Figure 3* SEM photographs of carbonized fibres spun through nozzles of different dimensions.

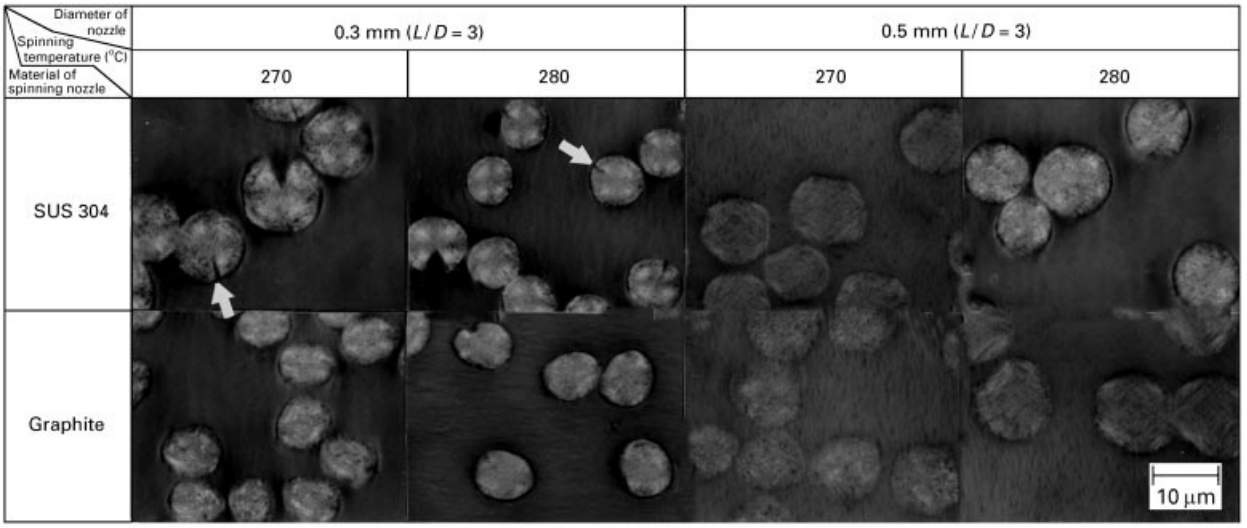


*Figure 4* Optical micrographs of carbonized fibres at 600 °C spun through nozzles made of SUS 304 and graphite [ISO-88-3000 (Tokyo Carbon Co.): density, 1.90 g cm$^{-3}$; share strength, 90; conductivity, 1500 μΩ cm; compressive strength, 1850 kgf cm$^{-2}$; CTE ($\times 10^{-6}$), 6.5; thermal conductivity, 60 kcal nm °C].

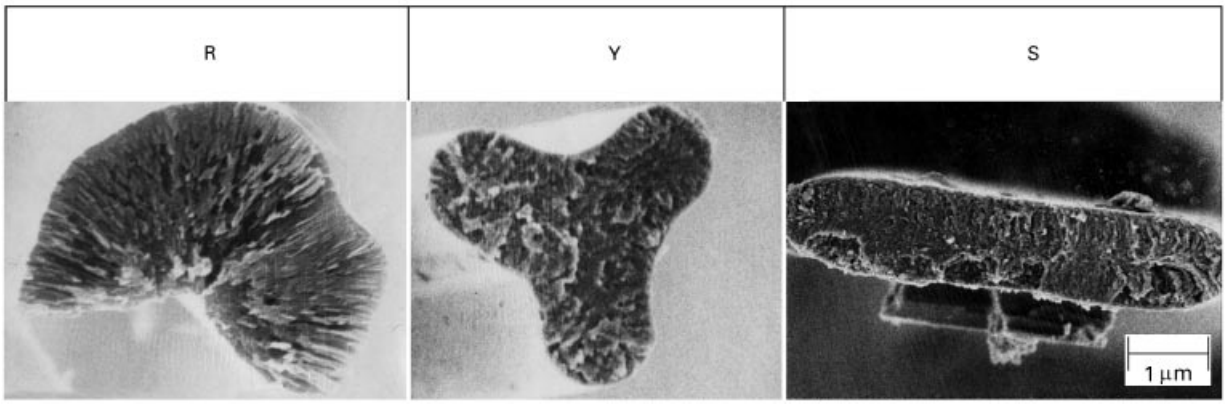


*Figure 5* SEM photographs of carbonized fibres spun through different shaped nozzles. Conditions of preparation: 1, mesophase pitch, mNP; 2, spinning temp., 275 °C; 3, stabilization, 270 °C, 30 min, 5 K min$^{-1}$; 4, carbonization, 1300 °C, 60 min, 10 K min$^{-1}$.

$D = 0.3$ mm), slit ($0.1 \times 0.7$ mm) and Y-shaped SUS nozzles. All graphitized fibres exhibited typical radial textures in transverse section where the domains were aligned perpendicularly to the fibre surface; however, only the fibre spun through the round-shaped nozzle provided open cracks in transverse sections. Transverse domains of round-shaped fibres were concentrated on a centre point, exhibiting one-point symmetry. The domains perpendicularly aligned to the surface penetrated almost into the centre of the trilobal and slit-shaped fibres, although the detailed alignment was more complex (as reported previously), with no point symmetry being found [10].

## 3.4. Nature of mesophase pitches

Fig. 6 shows the transverse sections of the graphitized fibres from mNP, NP and C9/mNP blends spun through the round-shaped SUS nozzle at 275–285 °C to give the same viscosities. All mNP fibres provided typical radial open cracks as described before. In contrast, NP ones exhibited radial skin-random core textures, carrying shallow cracks in some fibres ($< 10\%$). Fibres from C9/mNP blends showed a skin-onion–core radial texture, carrying no open crack.

## 3.5. Longitudinal alignment along the fibre axis

Fig. 7 illustrates the degree of preferred orientation along the axis of the mNP fibre spun at several temperatures through the SUS and graphitized nozzles of $L/D = 3$ and $D = 0.3$ mm. The preferred orientation increases with increased spinning temperature, up to 285 °C where the extent became maximum. Further higher spinning temperatures slightly reduced the preferred orientation. Although the SUS and graphite nozzles provide similar changes of the preferred orientations, according to the spinning temperature, the graphite nozzle certainly reduced the preferred orientation.

The degree of preferred orientation of NP fibres are also illustrated in Fig. 7, when the SUS nozzle was applied. Although a similar profile to that of the mNP fibre was obtained, the preferred orientations of the NP fibres exhibited lower orientation.

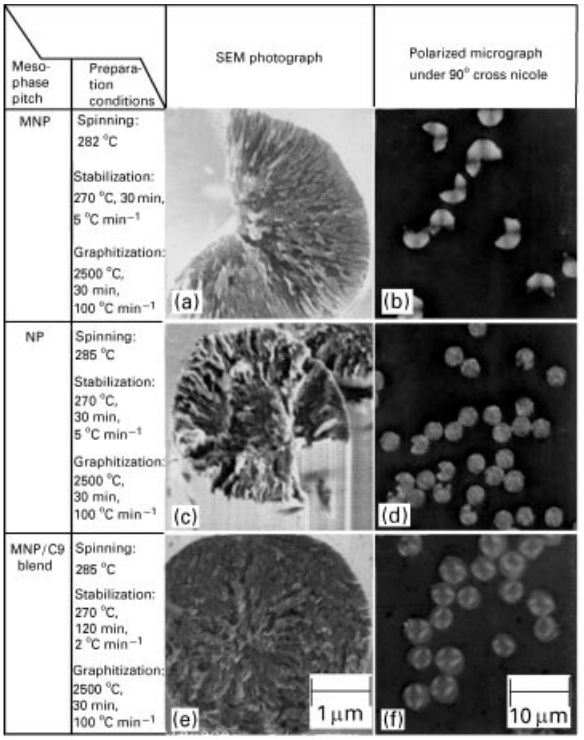


*Figure 6* SEM and OM photographs of graphitized fibres derived from mNP, NP and a C9/mNP blend. (a) SEM photograph of graphitized fibre from mNP; (b) OM photograph of graphitized fibre from mNP; (c) SEM photograph of graphitized fibre from NP; (d) OM photograph of graphitized fibre from NP; (e) SEM photograph of graphitized fibre from C9/mNP blend; (f) OM photograph of graphitized fibre from C9/mNP blend.

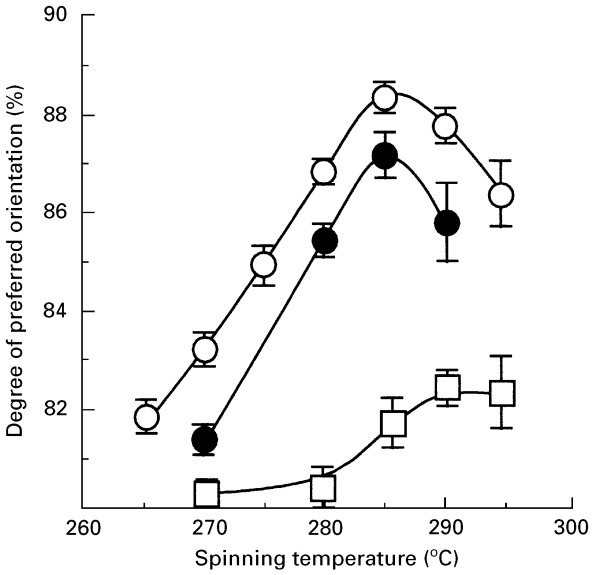


*Figure 7* The degree of preferred orientation of as-spun fibres. ○, As-spun fibres from mNP spun through SUS-304 nozzle ($D = 0.3$ mm, $L/D = 3$); ●, as-spun fibres from mNP spun through graphite nozzle ($D = 0.3$ mm, $L/D = 3$); □, as-spun fibre from NP spun through SUS-304 nozzle ($D = 0.3$ mm, $L/D = 3$).

## 4. Discussion

The present study reveals the steps of development of open-wedge cracks at spinning, stabilization, carbonization, calcination and graphitization. Spinning aligns the domains of mesogen assemblies in the mesophase into the radial texture of domain distribution [11]. The as-spun fibre of radial texture already carried an embryo of a small crack, which ran from the surface to the centre. The stabilization fixes the texture so that it cannot change during the successive carbonization, while the crack increases its open angle in some textures during stabilization. Carbonization and graphitization allow the growth and closer stacking of the hexagonal carbon planes in the fibre according to the alignment of mesogen planes in the domains. Thus, the domains aligned in the radial texture are densified through graphitic shrinkage according to the evolution of volatile matters and gases and the reduction of d-spacing, leading to their shrinkage in the circumferential direction to broaden the angle of crack. The graphitization further reduces the d-spacing and thickness of domain, further broadening the crack. In a particular case, as shown in Fig. 2d, the crack became semi-spherical.

Such crack development depends on the transverse texture of domains. Hence, each domain should shrink circumferentially with the other domains to develop the crack, otherwise no crack broadening takes place. The domain has been revealed to have several shapes [11]. The detailed definition of the domain shape and its arrangement should be correlated with crack development, since some fibres of radial texture, defined by an optical microscope, exhibited no crack, or narrow and/or shallow cracks. Detailed classification of the radial texture will be reported in a successive paper, based on observations by high resolution scanning electron microscopy (HR-SEM).

The other structural parameter of the fibre related to the development of the crack is the degree of preferred orientation of the as-spun fibre, as shown in Fig. 7. The highest preferred orientation observed at the highest temperature gave a radial texture with the largest crack. Since the crack runs along the fibre axis, such a correlation appears reasonable.

It is of value to point out that the alignment of domains perpendicular to the fibre surface (radial texture) does not always lead fibres to the open crack, as observed in the trirobal and slit-shaped fibres. The texture with a point symmetry which allows circumference shrinkage is essential to crack development.

The spinning conditions certainly define the alignment of domains, hence they are very influential on crack formation. So far $L/D$ of nozzle dimension and spinning temperature have been pointed out to influence crack formation [2, 3]. The present study recognized their influence in more detail. Large $L/D$ tend to give larger cracks by spinning over a particular range of temperatures. The diameter and wall material of the nozzle are also found to be influential on crack development. The graphite wall reduced the preferred orientation, with no crack being produced. Influence of spinning temperature was found to be non-monotonous, although the viscosity should decrease monotonously at higher temperatures. The lowest temperature of spinning provided radial textures with no cracks. Higher temperatures increased the chance and angle of crack up to a particular temperature where the radial texture is still induced and the highest

preferred orientation is achieved. Further higher temperatures provided no further radial texture and no crack.

The transverse texture certainly changes with temperature. The importance of apparent viscosity should be emphasized to define the details of texture and preferred orientation that are most influential on crack formation. The apparent viscosity is influenced by shear rate as well as temperature [12]. The smaller viscosity is easy to complete the radial texture from the surface to the centre, giving the higher preferred orientation, both of which provide more chance of crack formation. The spinning temperature also influences the die-swelling at the outlet of the spinning spinneret which can modify the radial alignment achieved in the nozzle [13]. The higher temperature tends to allow such a die-swelling because higher temperatures provide larger elastic moduli [14] and a longer period of melt state to provoke the flow properties of the mesophase pitch at the outlet of the spinning spinneret (as discussed previously [13]). Thus, the highest temperature where the die-swelling does not change radial alignment into a skin-onion provides the perfect radial texture and the highest preferred orientation suitable for the formation of the largest crack.

The mesophase pitches have been recognized to exhibit structure-dependent viscosity [13]. The present authors have pointed out very different shear rate–viscosity correlation of NP and mNP derived mesophase pitches; mNP exhibited very strong reduction of apparent viscosity by shear through the slippage of the stacked molecules [12]. Thus, mNP provides radial textures of highly preferred orientations along the fibre axis, tending to exhibit the open-wedge crack. The rapid cooling of the mesophase pitch prevents die-swelling and texture modification at higher spinning temperatures [13]. Such properties are suggested to reflect its higher stacking in the liquid state even at the spinning temperature. Mesophase pitch derived from C9 hydrocarbons provided the fibre with quasi-onion transverse texture at the higher spinning temperature of 280 °C [15], while mNP provided the fibre with a radial open crack texture. Their blends provided the very special onion skin–radial core texture, carrying no open cracks. Phase separation of mNP and C9 mesophase components was supposed to take place in the spinning capillary at the spinning step. Such a phase separation may provide a C9-rich region in the skin part and an mNP-rich part in the centre, resulting in the special onion skin–radial core transverse texture.

## References


1. M. MATSUMOTO, T. IWASHITA, Y. ARAI and T. TOMIOKA, *Carbon* **31** (1993) 715.
2. T. MATSUMOTO, *Pure Appl. Chem.* **57** (1985) 1553.
3. Y. YAMADA and H. HONDA, Japanese Patent Kokai 59-53713 (1984).
4. I. MOCHIDA, H. TOSHIMA, Y. KORAI and T. MATSUMOTO, *J. Mater. Sci.* **24** (1989) 57.
5. I. MOCHIDA, K. SHIMIZU, Y. KORAI, Y. SAKAI, H. OTSUKA and S. FUJIYAMA, *Carbon* **28** (1990) 311.
6. Y. KORAI, M. NAKAMURA, I. MOCHIDA, Y. SAKAI and S. FUJIYAMA, *ibid.* **29** (1991) 561.
7. K. YANAGIDA, T. SASAKI, H. YOSHIDA and K. TATE, Preprint of 16th Annual Meeting, The Carbon Society of Japan (Tokyo, Japan, 1989) p. 38.
8. F. FORTIN, S. H. YOON, Y. KORAI and I. MOCHIDA, *Carbon*, in press.
9. Japan Society for Promotion of Science (JSPS), *TANSO* **36** (1963) 25 (in Japanese).
10. *Idem.*, Extended Abstracts of Biennial Conference on Carbon, Buffalo, NY (1993) p. 248.
11. S. H. YOON, F. FORTIN, N. TAKANO, Y. KORAI and I. MOCHIDA, Proceedings of International Symposium on Carbon, Granada, Spain (1994) p. 682.
12. S. H. YOON, Y. KORAI, I. MOCHIDA and H. KATO, *Carbon* **32** (1994) 273.
13. S. H. YOON, Y. KORAI and I. MOCHIDA, *ibid.* **31** (1993) 849.
14. T. CHEUNG and B. RAND, in Proceedings of International Symposium on Carbon, Granada, Spain, 1994, p. 736.
15. I. MOCHIDA, S. H. YOON, F. FORTIN and Y. KORAI, Workshop on Carbon Materials for Advanced Technologies (ACS, Washington DC, USA 1944).



*Received 12 October 1994*
*and accepted 13 February 1996*